Catalysis Communications 127 (2019) 69–74

Contents lists available at ScienceDirect

Catalysis Communications

journal homepage: www.elsevier.com/locate/catcom

Short communication

Heterogeneous catalytic decarboxylative sulfonylation of cinnamic acids with sodium benzene sulfinates over a manganese(II)-based rod-shaped metal-organic framework catalyst

Qi-Da Ding[a], Jin-Ping Si[a], Kun-Lin Huang[b], Feng Tian[a], Sheng-Chun Chen[a,*], Xue-Jun Feng[a], Ming-Yang He[a], Qun Chen[a,*]

[a] *Jiangsu Key Laboratory of Advanced Catalytic Materials and Technology, Changzhou University, Changzhou 213164, China*
[b] *College of Chemistry, Chongqing Normal University, Chongqing 401331, China*

ARTICLE INFO

Keywords:
Mn(II) MOF
Heterogeneous catalysis
Decarboxylative sulfonylation
Cinnamic acid
Vinyl sulfones

ABSTRACT

Based on the acid-base mixed-ligand assembly strategy, a stable Mn(II)-based metal-organic framework (denoted as Mn-MOFs), containing 1-D Mn–O–C rod-shaped chains, was hydrothermally synthesized and structurally characterized. This material was demonstrated to be an efficient heterogeneous catalyst for the decarboxylative sulfonylation of cinnamic acids with sodium benzene sulfinates. Moreover, the Mn-MOF catalyst could be recycled up to six times with the retention of both catalytic activity and crystal structure.

1. Introduction

Vinyl sulfones not only occur as important structural scaffolds in many biologically and medically active compounds [1], but also are the prevalent molecular fragment for various organic transformations [2,3]. The development of efficient methods for the synthesis of vinyl sulfones has attracted much attention in recent years [4–6]. In particular, transition-metal-catalyzed decarboxylative C–S cross-coupling reactions have emerged as one of the most powerful synthetic routes because a variety of carboxylic acids are extremely available raw materials for chemical synthesis [7–12]. Generally, this type of reaction proceeds in homogenous systems using transition-metal salts as catalysts, such as $Pd(OAc)_2$ [13], $Cu(ClO_4)_2$ [14] and $Mn(OAc)_2$ [15]. However, a major drawback of these homogeneous procedures is the resulting difficulty associated with separation and recycling of metal catalysts. To solve these problems, from an economical and sustainable point of view, developing highly efficient heterogeneous catalysts for decarboxylative sulfonylation is of great importance.

Metal-organic frameworks, consisting of organic linkers and metal-connecting nodes, have recently developed into an important class of crystalline materials for heterogeneous catalysis [16]. In MOF-based catalytic materials, the active sites might be introduced into MOFs through four possible ways: (1) unsaturated metal sites (UMS) at the nodes; (2) active sites embedded within the organic linkers and considered as part of the framework; (iii) active sites attached to metal nodes or organic linkers by post-synthetic modification method, and (iv) other active catalysts supported or encapsulated inside MOF cavities [17]. Particularly, UMS in MOFs can show various well-defined inorganic connectivities, ranging from discrete zero-dimensional moieties (mono-, di- and polynuclear species), one-dimensional inorganic chains, two-dimensional inorganic layers, even to three-dimensional inorganic hybrids [18]. In recent years, the use of active UMS with diverse inorganic connectivities toward enhanced heterogeneous organic transformations have been reported [19,20]. However, in most cases, the inferior thermal and chemical stability of MOFs leads to the collapse of the framework structure during the catalytic process. To address this problem, several groups have developed acid-base mixed-linker systems to construct MOF materials that exhibit higher stability and catalytic activity over those with one single organic linker [21,22]. Very recently, we have also shown the application of mixed-linker MOFs of Cu(II) and Co(II) as robust heterogeneous catalysts for the alcohol oxidation and cross-dehydrogenative coupling amination reactions [23,24].

Several studies have been conducted on the utilization of manganese salts and conventional solid-supported manganese oxide materials for catalytic decarboxylative couplings [4,15,25]. Over the past decade, Mn(II)-based MOFs have shown great promise as highly efficient heterogeneous catalysts for some important organic transformations [26–28]. In this communication, we used the mixed linkers of 1,4-naphthalenedicarboxylic acid (1,4-H_2NDC) and 1,4-bis(imidazol-1-ylmethyl)-2,3,5,6-tetrafluorobenenze (Fbix) to synthesize a stable Mn(II)-

---

[*] Corresponding authors.
E-mail addresses: csc@cczu.edu.cn (S.-C. Chen), chenqunjpu@yahoo.com (Q. Chen).

https://doi.org/10.1016/j.catcom.2019.05.006
recibido en 1 febrero 2019; recibido en versión revisada en 2 mayo 2019; aceptado en 7 mayo 2019
Available online 08 May 2019
1566-7367/ © 2019 Elsevier B.V. All rights reserved.

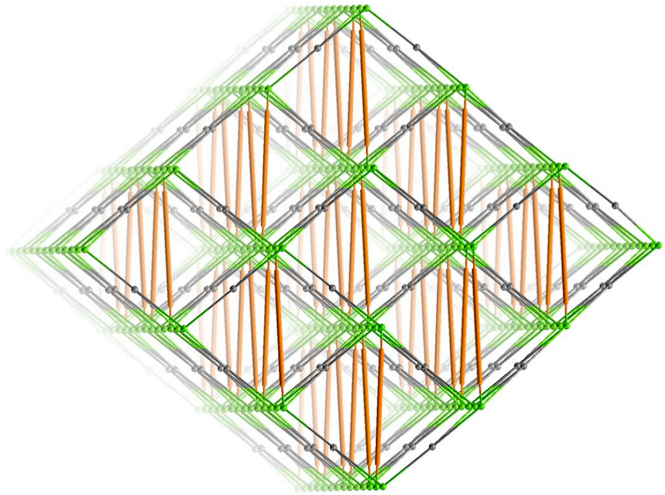

Fig. 1. Perspective view of the **hex**-type framework of Mn-MOF.

based rod-shaped MOF $[Mn_2(1,4\text{-}NDC)_2(Fbix)]_n$ (Mn-MOF), and applied it as an active and recyclable catalyst for the decarboxylative sulfonylation of cinnamic acids with sodium benzene sulfinates. Moreover, to our knowledge, catalytic decarboxylative sulfonylation reactions over MOF catalysts have not been mentioned in the literature.

2. Experimental

2.1. Catalyst synthesis

A mixture of $MnCl_2·4H_2O$ (39.6 mg, 0.2 mmol), 1,4-H_2NDC (21.6 mg, 0.1 mmol), Fbix (31.0 mg, 0.1 mmol) and water (7 mL) was stirred for 20 min at room temperature and then sealed in a 25-mL Teflon-lined stainless steel container, which was heated at 140 °C for 48 h. After cooling to room temperature, yellow block-shaped crystals were obtained in *ca.* 54.2% yield. The crystals were grinded, and washed with ethanol, and then dried in air, affording the powder used for the catalytic reactions.

The crystallographic data for Mn-MOF has been deposited as CCDC-1496990.

2.2. Catalytic reaction

In a typical experiment, cinnamic acid (74.1 mg, 0.5 mmol), sodium benzenesulfinate (246.2 mg, 1.5 mmol), Mn-MOF (12.7 mg, 3 mol%), KI (249.0 mg, 3 equiv) and DMSO (4 mL) were taken in a 25-mL three-necked round-bottom flask. The solution was magnetically stirred for some hours at 110 °C under air atmosphere. The progress of the reaction was monitored by high-performance liquid chromatography (Shimadzu LC-VP) with a UV detector at 274 nm, a Hypersil ODS2 column (250 mm × 4.6 mm, 5 μm), and a mixture of CH_3CN and H_2O (*v*/v: 6:4) as eluent. The concentration of cinnamic acid and product were calibrated by external standard method with standard samples. The reaction solution containing Mn-MOF catalyst was easily separated by filtration, and the catalyst was then washed with DMSO and ethanol and dried under vacuum.

3. Results and discussion

3.1. Synthesis and characterization of catalyst

Both 1,4-H_2NDC and Fbix are insoluble in water at room

Table 1
Optimization of the reaction conditions[a].

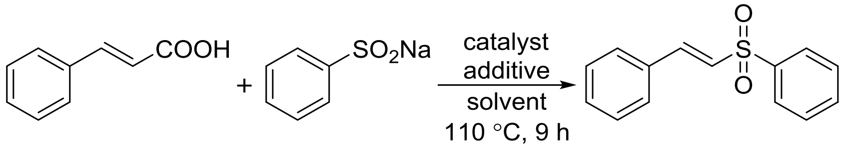

Entry	Catalyst	Additive	Solvent	Yield (%)[b]
1	Mn-MOF	KI	DMSO	93
2	Mn-MOF	KI	DMA	81
3	Mn-MOF	KI	DCE	64
4	Mn-MOF	KI	DMF	80
5	Mn-MOF	KI	NMP	72
6	Mn-MOF	KI	H_2O	16
7	Mn-MOF	KI	EtOH	18
8	Mn-MOF	None	DMSO	28
9	Mn-MOF	NaI	DMSO	68
10	Mn-MOF	NH_4I	DMSO	31
11	Mn-MOF	I_2	DMSO	Trace
12	Mn-MOF	K_2CO_3	DMSO	Trace
13	Mn-MOF	KCl	DMSO	46
14	Mn-MOF	KBr	DMSO	73
15	None	KI	DMSO	8
16[c]	Mn-ZSM-5	KI	DMSO	28
17[d]	Mn/SiO_2	KI	DMSO	35
18[e]	Mn/Sil-1-10-2	KI	DMSO	32
19[f]	Mn-MOF	KI	DMSO	15

[a] Reaction conditions: cinnamic acid (0.5 mmol), sodium benzenesulfinate (1.5 mmol), additive (3.0 equiv), catalyst (12.7 mg, 3 mol% Mn), solvent (4.0 mL), under air.

[b] Based on LC analysis.

[c] With 105.6 mg Mn-ZSM-5 (3 mol% Mn).

[d] With 41.2 mg Mn/SiO_2 (3 mol% Mn).

[e] With 41.2 mg Mn/Sil-1-10-2 (3 mol% Mn).

[f] Under N_2.

Table 2
Substrate scope for the synthesis of vinyl sulfones[a, b].

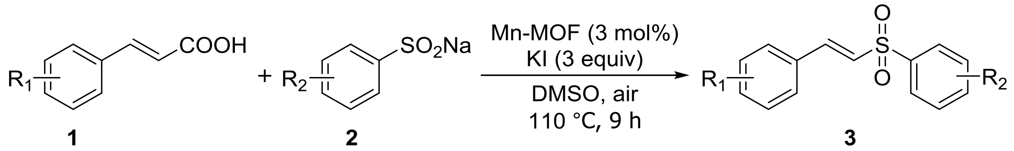

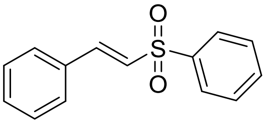

3a: 93%

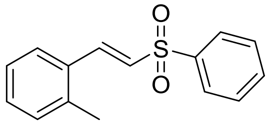

3b: 86%

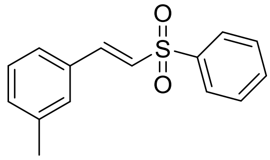

3c: 94%

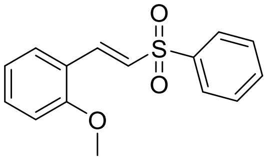

3d: 92%

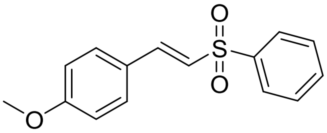

3e: 88%

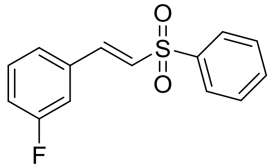

3f: 72%

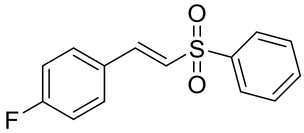

3g: 77%

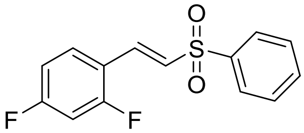

3h: 42%

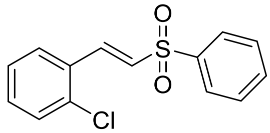

3i: 70%

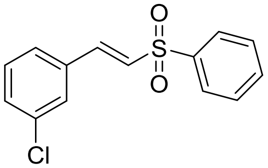

3j: 64%

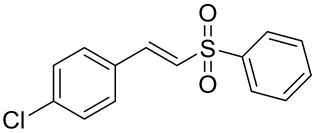

3k: 75%

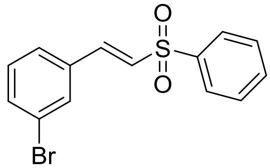

3l: 65%

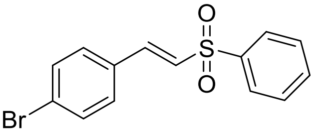

3m: 72%

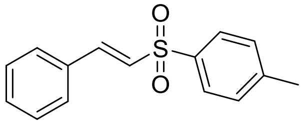

3n: 98%

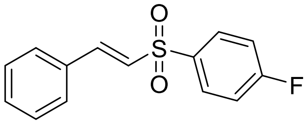

3o: 96%

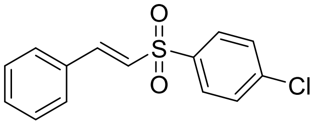

3p: 84%

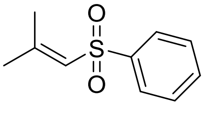

3q: n.d

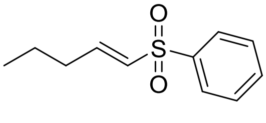

3r: n.d

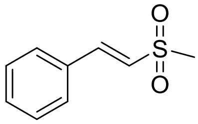

3s: n.d

---

[a] Reaction conditions: **1** (0.5 mmol), **2** (1.5 mmol), KI (1.5 mmol), DMSO (4 mL), Mn-MOF (12.7 mg, 3 mol% Mn), 110 °C, 9 h, open air. [b] The yields are of materials isolated by column chromatography.

temperature. Mn-MOF was prepared under hydrothermal conditions in a moderate yield. It should be pointed out that only amorphous powder was obtained under similar reaction conditions when manganese(II) salts including $Mn(OAc)_2 \cdot 2H_2O$ and $MnSO_4 \cdot H_2O$.

Single-crystal X-ray diffraction analysis revealed that Mn-MOF crystallizes in the monoclinic space group $P2_1/c$ and the asymmetric unit contains two Mn(II) ions (Mn1 and Mn2), two 1,4-NDC anions, and one Fbix ligand. Both Mn1 and Mn2 are five-coordinated by four oxygen atoms from four 1,4-NDC ligands with the Mn–O distances in the range of 2.036(2)–2.168(2) Å and one nitrogen atom from Fbix ligand with the Mn–N distances of 2.187(2) and 2.236 Å, exhibiting a distorted square-pyramid geometry (Fig. S1). Each 1,4-NDC ligand is linked to four Mn(II) ions with two carboxylate groups adopting the μ_2-η^1:η^1-*syn*-syn-bridging mode. Adjacent Mn(II) ions are linked in sequence by carboxylate groups of 1,4-NDC, forming an 1-D Mn–O–C rod-shaped chains along the *c*-axis (Fig. S2). Each chain links four neighboring chains through the 1,4-NDC linkers to generate a 3-D sub framework (Fig. S3). The Fbix ligand exhibits a *trans* configuration and connects the rod-shaped chains together with 1,4-NDC to form the final 3-D framework with the **hex** net (Figs. 1 and S4) [29].

Powder X-ray diffraction (PXRD) patterns (Fig. S5) confirmed the phase purity of the as-synthesized Mn-MOF. The thermal stability was investigated by the combination of TG analysis and temperature-dependent PXRD patterns (Figs. S6 and S7), suggesting that Mn-MOF can retain its structure in air up to 300 °C. Moreover, after the bulk samples were suspended in refluxing water, ethanol, dichloroethane or hot organic solvents including DMF, NMP and DMSO at 120 °C for 24 h, Mn-MOF could remain intact without loss of crystallinity (Fig. S8).

3.2. Catalytic performance

The decarboxylative sulfonylation of cinnamic acid with sodium benzene sulfinate was selected as a model reaction using Mn-MOF as heterogeneous catalyst to study the reaction conditions. First, a screening of different solvents revealed that aprotic polar solvents gave higher yields, where DMSO was found to be the best (Table 1, entries 1–7). On the basis of the $Mn(OAc)_2$-catalyzed decarboxylative sulfonylation reported by Deng et al. [15,30–32], the iodine additive is crucial for this reaction. Then, influence of various reagents on the reaction was investigated. In the absence of the iodine reagent, the reaction gave a low yield (entry 8). Significantly enhanced yield was observed in the presence of KI, and addition of other additives including I_2 and K_2CO_3 failed to give any positive effect (entries 11 and 12). Furthermore, when KCl and KBr were employed instead of KI, the reactions could proceed smoothly to afford the corresponding product in moderate to good yields (entries 13 and 14). The results suggested that iodide anion might act as soft Lewis base to capture soft Lewis acid carbon cation in this transformation, giving the corresponding vinyl sulfone products with high yields, which is similar to that observed in the heterogeneous catalytic process reported by Guo et al. [8]. It was also found that the reaction in the absence of Mn-MOF catalyst gave only trace product (entry 15), while the yield was dramatically improved to 93% when 3 mol% Mn-MOF was added to the reaction mixture. In our previous work, Cu-doped zeolites have been developed for decarboxylative coupling reactions [33]. For comparison, Mn-containing heterogeneous catalysts including Mn-ZSM-5, Mn/SiO_2 and Mn/Sil-1-10-2 in the reaction system were far less efficient (entries 16–18). Similar to the homogenous Mn(II)-catalyzed system [15], the presence of air atmosphere was beneficial to this transformation. When the reaction was conducted under N_2 atmosphere, yield was significantly diminished (entry 19).

Fig. S9 shows the dependence of the yield on the effect of reaction temperature. Indeed, the yield markedly increased at higher temperature and 110 °C was found to be a relatively optimized temperature, where the reaction could afford 93% yield after 9 h. Another factor that should be considered for the cross-coupling reaction over the Mn-MOF catalyst is the reagent molar ratio. A large excess of sodium benzenesulfinate should be required for the coupling. Fig. S10 shows the dependence of the yield on the effect of reagent molar ratio. At 3 mol% Mn-MOF loadings, higher yield was achieved at 110 °C when 3 equivalents of sodium benzenesulfinate were used, while utilization of lower amounts of sodium benzenesulfinate led to a obvious decrease in reaction efficiency.

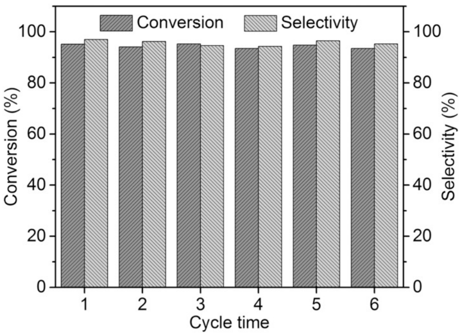

Fig. 2. Catalyst recycling studies.

Subsequently, the substrate scope of the Mn-MOF-catalyzed decarboxylative sulfonylation reaction was also explored with diverse substituted cinnamic acids and sodium benzenesulfinates under the above-mentioned optimal conditions (see Table 2). The Mn-MOF catalyst was found to efficiently catalyze a range of cinnamic acids and several sodium benzenesulfinates, and the products were isolated in yields ranging from 42% to 98%. Cinnamic acid derivatives bearing electron-donating functional groups afforded better yields than the substrates with electron-withdrawing substituents. Moreover, sodium benzenesulfinates with 4-H, 4-Me, 4-F and 4-Cl groups substituted on phenyl rings proceeded smoothly to give the desired vinyl sulfone products. Between *ortho-* and *meta*-methyl or chloride substituents, no obvious negative steric effect was found. In addition, aliphatic substrates such as 3-methyl-2-butenoic acid and trans-2-hexenoic acid as well as sodium methane sulfinate have also been examined for the catalytic system. However, no desired products were obtained.

3.3. Catalyst heterogeneity and reusability

To verify the heterogeneous nature of the Mn-MOF-catalyzed reaction process, the leaching experiments were carried out (Fig. S9). After removing the solid catalyst, it was found that no further conversion of cinnamic acid was detected even after 8 h. Moreover, examination by ICP analysis of the filtrate indicated a negligible amounts ($<$ 1 ppm) of the manganese. In recycling tests, before the catalyst was reused, the Mn-MOF catalyst was collected by centrifugation, washed with DMSO and ethanol, and dried at 60 °C under vacuum in 12 h. The results revealed that the recovered Mn-MOF catalyst could almost maintain its high activity with no decrease after six consecutive cycles (Fig. 2). Furthermore, the PXRD pattern of 6th used catalyst indicated that the Mn-MOF could retain its crystallinity (Fig. S10).

3.4. Proposed mechanism

To understand the reaction pathway better, some control experiments were carried out (Scheme 1). The reaction of **1a** with **2a** was conducted under the standard reaction conditions in the presence of radical scavengers, including 2,6-di-tert-butyl-4-methylphenol (BHT) and 2,2,6,6-tetramethyl-1-piperidinyloxy (TEMPO) (Scheme 1a and b). BHT was found to suppress the reaction while TEMPO totally stopped the reaction, which implied that a radical pathway should be involved. Next, when styrene was employed as a substrate in place of **1a** (Scheme 1c), no **3a** was observed. The result suggested that styrene is not an intermediate in the present reaction. Furthermore, it was also found

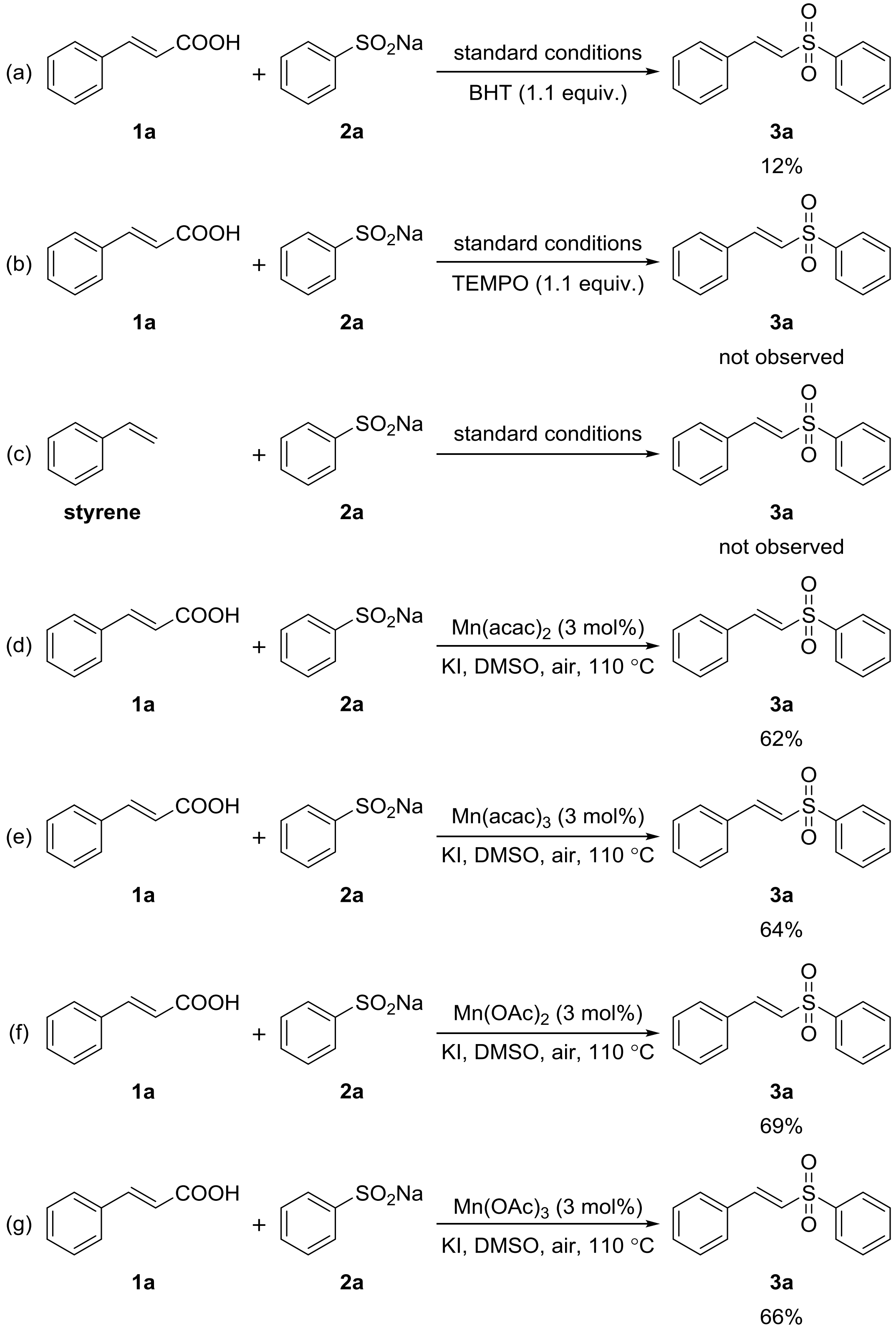

Scheme 1. Control experiments.

that the homogeneous Mn(II) catalysts (Scheme 1d and f)and Mn(III) species (Scheme 1e and g) showed comparable activity, suggesting that the true catalyst might be the Mn(III) species [15]. Comparison of catalytic activities of the Mn(II) and Mn(III) catalysts in the model reaction with that of Mn-MOF revealed that Mn-MOF exhibits higher performance, which may be related to the characteristic of the Mn-based rod-shaped active sites [34]. The oxidation state of manganese species in the fresh Mn-MOF and the samples of different catalytic cycles have been analyzed by X-ray photoelectron spectroscopy (XPS) (Fig. S14). The observation of the Mn $2p_{3/2}$ peak at 643.20 eV demonstrated no change in the oxidizing state for manganese, further implying Mn-MOF is stable during the reaction process. To detect the

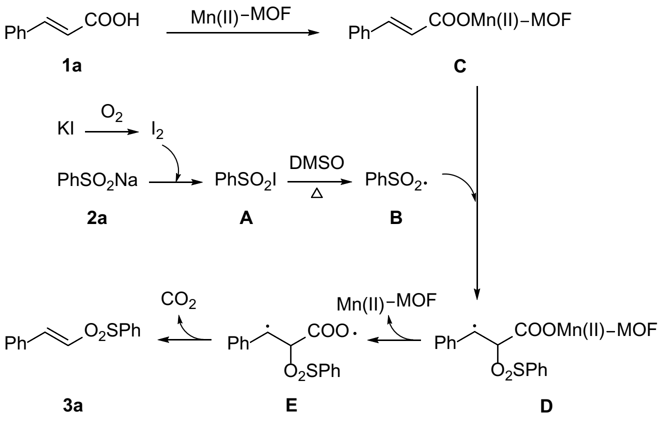

Scheme 2. Proposed reaction mechanism.

possible intermediates, after conducting the reaction for 30 min, the ESI-MS spectrum of the reaction mixture was measured (Fig. S15). The most revealing signal is found at $m/z = 267.04$ (relative intensity = 100%), which might match the specie of sulfone + Na+.

On the basis of these results, we propose the tentative mechanism shown in Scheme 2. First, KI is converted to I_2 under oxidation conditions, and the reaction of sodium benzenesulfinate with I_2 generates sulfonyl iodide **A**, which is dissociated into sulfonyl radical **B**. Simultaneously, the cinnamic acid substrate reacts with the Mn(II)-MOF to form the Mn(II)-MOF intermediate **C**, involving initial coordination of carboxylic acid to the Mn(II) ion. Subsequently, the radical **B** attacks the intermediate **C** at the α-carbon to furnish intermediate **D**, which is transformed into the biradical intermediate **E** *via* the homolysis of the Mn(II)-carboxylate bond. Finally, the **E** would undergo the loss of one molecule of CO_2 to afford the target product **3a**.

4. Conclusion

In summary, a new stable Mn(II)-based MOF catalyst was hydrothermally synthesized using the mixed-ligand synthetic strategy. The MOF material is a rare example of **hex**-type framework consisting 1-D Mn–O–C rod-shaped sites, and could serve as a highly active and recyclable catalysts for the decarboxylative sulfonylation of cinnamic acids with sodium benzene sulfinates. This work highlights the feasibility of using Mn(II)-based mixed-ligand MOFs as heterogeneous catalysts for decarboxylative coupling reactions.

Acknowledgements

This research was supported by the National Natural Science Foundation of China (21676030), a Project Funded by the Priority Academic Program Development of Jiangsu Higher Education Institutions (PAPD), the Advanced Catalytic and Green Manufacturing Collaborative Innovation Center, Changzhou University and Jiangsu Key Laboratory of Advanced Catalytic Materials and Technology (ZZZD201807 and BM2012110).

Appendix A. Supplementary data

Supplementary data to this article can be found online at https://doi.org/10.1016/j.catcom.2019.05.006.

References

[1] D.C. Meadows, J. Gervay-Hague, Med. Res. Rev. 26 (2006) 793–814.
[2] T.G. Back, K.N. Clary, D. Gao, Chem. Rev. 110 (2010) 4498–4553.
[3] A. Hosseinian, P.D.K. Nezhad, S. Ahmadi, Z. Rahmani, A. Monfared, J. Sulfur Chem. 40 (2019) 88–112.
[4] S. Waiba, M.K. Barman, B. Maji, J. Organomet. Chem. 84 (2019) 973–982.
[5] M. Ratushnyy, M. Kamenova, V. Gevorgyan, Chem. Sci. 9 (2018) 7193–7197.
[6] S. Mao, Y.-R. Gao, X.-Q. Zhu, D.-D. Guo, Y.-Q. Wang, Org. Lett. 17 (2015) 1692–1695.
[7] S. Li, X. Li, F. Yang, Y. Wu, Org. Chem. Front. 2 (2015) 1076–1079.
[8] Q. Jiang, B. Xu, J. Jia, A. Zhao, Y.-R. Zhao, Y.-Y. Li, N.-N. He, C.-C. Guo, J. Organomet. Chem. 79 (2014) 7372–7379.
[9] Y. Xu, X. Tang, W. Hu, W. Wu, H. Jiang, Green Chem. 16 (2014) 3720–3723.
[10] P. Qian, M. Bi, J. Su, Z. Zha, Z. Wang, J. Organomet. Chem. 81 (2016) 4876–4882.
[11] S. Cai, Y. Xu, D. Chen, L. Li, Q. Chen, M. Huang, W. Weng, Org. Lett. 18 (2016) 2990–2993.
[12] P. Katrun, S. Hlekhlai, J. Meesin, M. Pohmakotr, V. Reutrakul, T. Jaipetch, D. Soorukram, C. Kuhakarn, Org. Biomol. Chem. 13 (2015) 4785–4794.
[13] R. Guo, Q. Gui, D. Wang, Z. Tan, Catal. Lett. 144 (2014) 1377–1383.
[14] B.V. Rokade, K.R. Prabhu, J. Organomet. Chem. 79 (2014) 8110–8117.
[15] N. Xue, R. Guo, X. Tu, W. Luo, W. Deng, J. Xiang, Synlett 27 (2016) 2695–2698.
[16] Y.-B. Huang, J. Liang, X.-S. Wang, R. Cao, Chem. Soc. Rev. 46 (2017) 126–157.
[17] P. Ryan, I. Konstantinov, R.Q. Snurr, L.J. Broadbelt, J. Catal. 286 (2012) 95–102.
[18] A.K. Cheetham, C.N.R. Rao, R.K. Feller, Chem. Commun. 46 (2006) 4780–4795.
[19] G. Lan, Z. Li, S.S. Veroneau, Y.-Y. Zhu, Z. Xu, C. Wang, W. Lin, J. Am. Chem. Soc. 140 (2018) 12369–12373.
[20] J. Ye, L. Gagliardi, C.J. Cramer, D.G. Truhlar, J. Catal. 354 (2017) 278–286.
[21] S. Yuan, J.-S. Qin, L. Zou, Y.-P. Chen, X. Wang, Q. Zhang, H.-C. Zhou, J. Am. Chem. Soc. 138 (2016) 6636–6642.
[22] A. Dhakshinamoorthy, A.M. Asiri, H. Garcia, Catal. Sci. Technol. 6 (2016) 5238–5261.
[23] S.-C. Chen, S.-N. Lu, F. Tian, N. Li, H.-Y. Qian, A.-J. Cui, M.-Y. He, Q. Chen, Catal. Commun. 95 (2017) 6–11.
[24] S.-C. Chen, N. Li, F. Tian, N.-N. Chai, M.-Y. He, Q. Chen, Mol. Catal. 450 (2018) 104–111.
[25] M. Gliński, J. Kijeński, Appl. Catal. A Gen. 190 (2000) 87–91.
[26] Y. Ha, M. Mu, Q. Liu, N. Ji, C. Song, D. Ma, Catal. Commun. 103 (2018) 51–55.
[27] Y.S. Raupp, C. Yildiz, W. Kleist, M.A. Meier, Appl. Catal. A Gen. 546 (2017) 1–6.
[28] H. Fei, M.D. Sampson, Y. Lee, C.P. Kubiak, S.M. Cohen, Inorg. Chem. 54 (2015) 6821–6828.
[29] B. Li, X. Zhou, Q. Zhou, G. Li, J. Hua, Y. Bi, Y. Li, Z. Shi, S. Feng, CrystEngComm 13 (2011) 4592–4598.
[30] J. Gao, J. Lai, G. Yuan, RSC Adv. 5 (2015) 66723–66726.
[31] J. Chen, J. Mao, Y. Zheng, D. Liu, G. Rong, H. Yan, C. Zhang, D. Shi, Tetrahedron 71 (2015) 5059–5063.
[32] S.J. Hwang, P.K. Shyam, H.-Y. Jang, Bull. Kor. Chem. Soc. 39 (2018) 535–539.
[33] S. Chen, Z. Shao, Z. Fang, Q. Chen, T. Tang, W. Fu, L. Zhang, T. Tang, J. Catal. 338 (2016) 38–46.
[34] D.H. Lee, S. Kim, M.Y. Hyun, J.-Y. Hong, S. Huh, C. Kim, S.J. Lee, Chem. Commun. 48 (2012) 5512–5514.